P–T Conditions and the Influence of Graphite on Pelitic Phase Relations in the Ballachulish Aureole, Scotland

by DAVID R. M. PATTISON

Department of Geology and Geophysics, University of Calgary, Calgary, Alberta T2N 1N4

(*Received 10 March 1988; revised typescript accepted 20 December 1988*)

ABSTRACT

Pressure–temperature conditions of pelites in the Ballachulish aureole, Scotland, have been determined from a calibrated petrogenetic grid and from published geothermometers and geobarometers. To calibrate the mineral reactions in the grid, thermodynamic data for appropriate end members of Ms, Chl, Qtz, And, Sil, Ky, Crn, Crd, Kfs, and Bt were derived from experimental data. This approach was hampered by the unknown compositions of many of the minerals used in the experiments, and by apparent inconsistency between the experiments. A best compromise grid that satisfies most of the data was obtained, which is applicable to the Ballachulish and other contact aureoles. In this grid, the first development of sillimanite is constrained to lie between the Richardson *et al.* (1969) and Holdaway (1971) andalusite–sillimanite boundaries.

A pressure estimate of $3{\cdot}0 \pm 0{\cdot}5$ kb is obtained from the calibrated grid, within 0·3 kb of estimates from geobarometry and from two other independent petrological studies. Temperatures ranged from 560 ± 20 °C at the first development of cordierite in the assemblage Ms + Qtz + Chl + Crd + Bt to 750–800 °C in Grt + Crd + Hy assemblages in pelitic screens within the igneous complex.

In graphitic slates, in contrast to non-graphitic pelites, an entire andalusite-bearing subzone is developed, and initial cordierite development occurs further from the igneous contacts. The presence of graphite lowered a_{H_2O} in the slates, expanding the stability field of the andalusite-bearing assemblage And + Qtz + Bt + Ms + Crd relative to the assemblage Kfs + Qtz + Bt + Ms + Crd developed in non-graphitic units. Initial development of cordierite in the assemblage Ms + Qtz + Chl + Crd + Bt was also promoted by reduced a_{H_2O} in graphitic slates.

The regular sequence and spacing of mineral zones in the aureole suggests that gross equilibrium was attained during contact metamorphism, even though the thermal metamorphic pulse is estimated to have been less than 0·2 Ma (Buntebarth, in press). There is no evidence for reaction overstepping in cordierite-producing reactions.

INTRODUCTION

The Ballachulish Igneous Complex and its contact metamorphic aureole have recently been the focus of a multidisciplinary investigation. Petrological, geochemical, isotopic, microstructural, and geophysical studies have addressed the mode of emplacement of the complex, origin of the magma, contact metamorphism and associated fluid movement, and kinetic controls of a variety of heterogeneous mineral reactions and mineral structural transformations (Voll *et al.*, in press).

This paper is the fourth in a series by the author on the contact metamorphism of pelitic rocks. Pattison & Harte (1985) described the petrology of the prograde sequence of assemblages in the aureole, rationalizing the assemblages in a petrogenetic grid in the model pelitic system K_2O–FeO–MgO–Al_2O_3–SiO_2–H_2O (KFMASH). Pattison (1987) documented a number of correlated chemical variations among the pelitic minerals going upgrade through the different zones, including Fe–Mg and (Fe, Mg)Si = 2Al. Pattison &

[*Journal of Petrology*, Vol. 30, Part 5, pp. 1219–1244, 1989]

Harte (1988) described the evolution of structurally contrasting anatectic migmatites adjacent to the contacts of the igneous complex.

This paper has three purposes: to calculate the P–T conditions of pelites in the aureole; to provide a simple explanation for the contrast in metamorphic response between graphitic and non-graphitic units; and to assess recent predictions that substantial overstepping of experimentally determined reaction boundaries is required to nucleate natural cordierite. In order to model the locations of the major end member reactions and to calculate the reaction positions for non-end member mineral and fluid compositions, an attempt was made to derive a simple internally consistent thermodynamic data set for the pelitic minerals in the aureole. This approach was taken because existing data sets were found to be unsatisfactory in modelling the reactions of interest. The derivation of the data is shown to be complicated both by the difficulties of estimating the unmeasured compositions of cordierite, biotite, muscovite, and chlorite used in the experiments (Holdaway, 1980), as well as by the apparent inconsistency of the experiments. Nevertheless, a best compromise model was found, which is used to construct quantitative P–T, T–X_{Fe-Mg} and T–a_{H_2O} diagrams applicable to the Ballachulish and other contact metamorphic aureoles.

At the highest grades in the aureole, rare garnet + cordierite + biotite ± hypersthene assemblages are found, allowing the application of Grt–Bt, Grt–Crd and Grt–Hy geothermometry and Grt–Hy–Pl–Qtz and Grt–Crd–Sil–Qtz geobarometry. The geobarometry is shown to be in excellent agreement with pressure estimates from the petrogenetic grid, but the geothermometry gives scattered results.

A conspicuous feature in the aureole is the contrast in metamorphic response between graphitic and non-graphitic rocks. In the graphitic rocks, an entire andalusite-bearing subzone is developed that is not seen in the non-graphitic units. In addition, initial cordierite is developed further out from the igneous contacts in graphitic rocks compared with non-graphitic units. These contrasts are accounted for by dilution of the hydrous vapour phase by C-bearing fluid species in the graphitic units.

Finally, Putnis & Holland (1986) argued that substantial overstepping of experimentally determined reaction boundaries is required to nucleate natural cordierite. It is argued here that there is no evidence for such overstepping, even in a rapidly heated contact aureole such as Ballachulish.

GEOLOGICAL SETTING

The Ballachulish Igneous Complex is a composite, 'I-type' pluton (Harmon, 1983). It is one of numerous post-tectonic plutonic bodies emplaced throughout the Scottish Caledonides at the end of the Caledonian Orogeny. Intrusion of the igneous complex postdated regional deformation and metamorphism of the Dalradian country rocks (Bailey & Maufe, 1960). The complex consists of a suite of grey diorites which is crosscut by an inner pink granite (Bailey & Maufe, 1960) (see Fig. 1). Moving outwards from the centre of the pluton, the grey diorites comprise a central orthopyroxene + clinopyroxene monzodiorite, a clinopyroxene + amphibole quartz diorite, and an amphibole + biotite quartz diorite (Weiss, 1989).

Rb–Sr whole-rock dating and K–Ar dating of biotite in the outer quartz diorite give a Lower Devonian age of 412 ± 28 Ma (Weiss, 1986). The emplacement temperature of the opx–cpx monzodiorite is estimated to have been 1100–1050 °C, and the crosscutting granite 850–800 °C (Weiss, 1986, 1989).

Three major Dalradian pelitic units enter the thermal aureole (Bailey & Maufe, 1960) (see Fig. 1): (1) interbedded pelitic, semipelitic, and calcareous rocks of the Appin Phyllite (A);

(2) the graphitic, sulphide-bearing Ballachulish Slate (B); and (3) phyllites, semipelites, striped siltstones, and dirty quartzites of the Leven Schist (L).

Regional metamorphic pelitic rocks outside of the aureole increase in grade from Ms + Chl + Qtz phyllites in the northwest of the map area to Ms + Grt + Bt + Qtz schists in the southeast. Estimated P–T conditions at the garnet isograd are 6 ± 1 kb and 470–510 °C (Pattison & Voll, in press).

THE BALLACHULISH AUREOLE

The geological map in Fig. 1 illustrates the location of the reaction boundaries between the different pelitic mineral zones in the aureole. The minerals and model Fe and Mg end member reactions that correspond to those in Fig. 1 are listed in Tables 1 and 2 respectively. Mineral abbreviations follow the scheme of Kretz (1983). Figure 2 shows the qualitative relationships between the reactions in a schematic petrogenetic grid in the model pelitic system KFMASH. The numbering system for the reactions in this paper follows that of Pattison & Harte (1985).

A number of lines of evidence suggest that the metamorphic field gradient in the Ballachulish aureole is isobaric. The Glen Coe and Lorne lavas, 10 km to the east and 15 km to the south, respectively, are essentially flat lying. These lavas, like the Ballachulish Igneous Complex, are Devonian in age (Evans *et al.*, 1971), which suggests that this part of the Southwest Highlands was uplifted without any major tilting since the Devonian. Droop & Treloar (1981), based on the field and geochemical evidence of Brown (1975), estimated a maximum tilting of 3 km over 35 km along a northwest–southeast axis in the Glen Etive Complex, 8 km to the southeast of Ballachulish. This would translate to a maximum variation of 0·7 km ($\sim$0·2 kb) across the 8 km width of the Ballachulish aureole, which is less than the 1 km relief in the area.

There is no evidence for downward or upward drag of country rock adjacent to the igneous contacts, such as has been suggested in models of buoyant diapiric ascent of granitoids by Marsh (1982). Rather, the principal mechanism of emplacement appears to have been stoping (Weiss, 1989). Bedding and regional structures with consistent attitudes are preserved right up to the contact, except for one part of the west contact which may have been affected by ballooning of the later granite (Pattison & Harte, 1988; Weiss & Troll, in press). Consequently, high-grade well-bedded rocks adjacent to the igneous contacts were probably at the same pressure as rocks further out in the aureole at the time peak metamorphic temperatures prevailed. The metamorphic field gradient in the aureole is thought to be virtually the same as the prograde P–T trajectory in the aureole, because of the relative brevity of the prograde thermal metamorphic pulse ($<$0·2 Ma) (Buntebarth, in press) relative to estimated Devonian uplift rates at the time (0·5 mm/a, Dempster, 1985).

Masch & Heuss-Assbichler (in press), in an independent study of calc-silicate reactions in the aureole, obtained a pressure estimate of $2{\cdot}8 \pm 0{\cdot}4$ kb, with temperatures increasing from $\sim$400 °C outside initial cordierite development in pelites to $\sim$750 °C at the igneous contact. Weiss & Troll (in press) estimated a pressure for crystallization of the igneous complex of 2·5–3·0 kb, based on the closeness in composition of late Pl + Kfs + Qtz granites to the 3 kb ternary minimum in the haplogranite system. These independent pressure estimates are shown to be in excellent agreement with pressure estimates from the pelites.

There is no evidence for the flow of meteoric or regional metamorphic fluids towards the igneous complex during contact metamorphism. In most of the aureole, abundant quartzo-feldspathic lithologies show little or no sign of anatexis even though temperatures were high

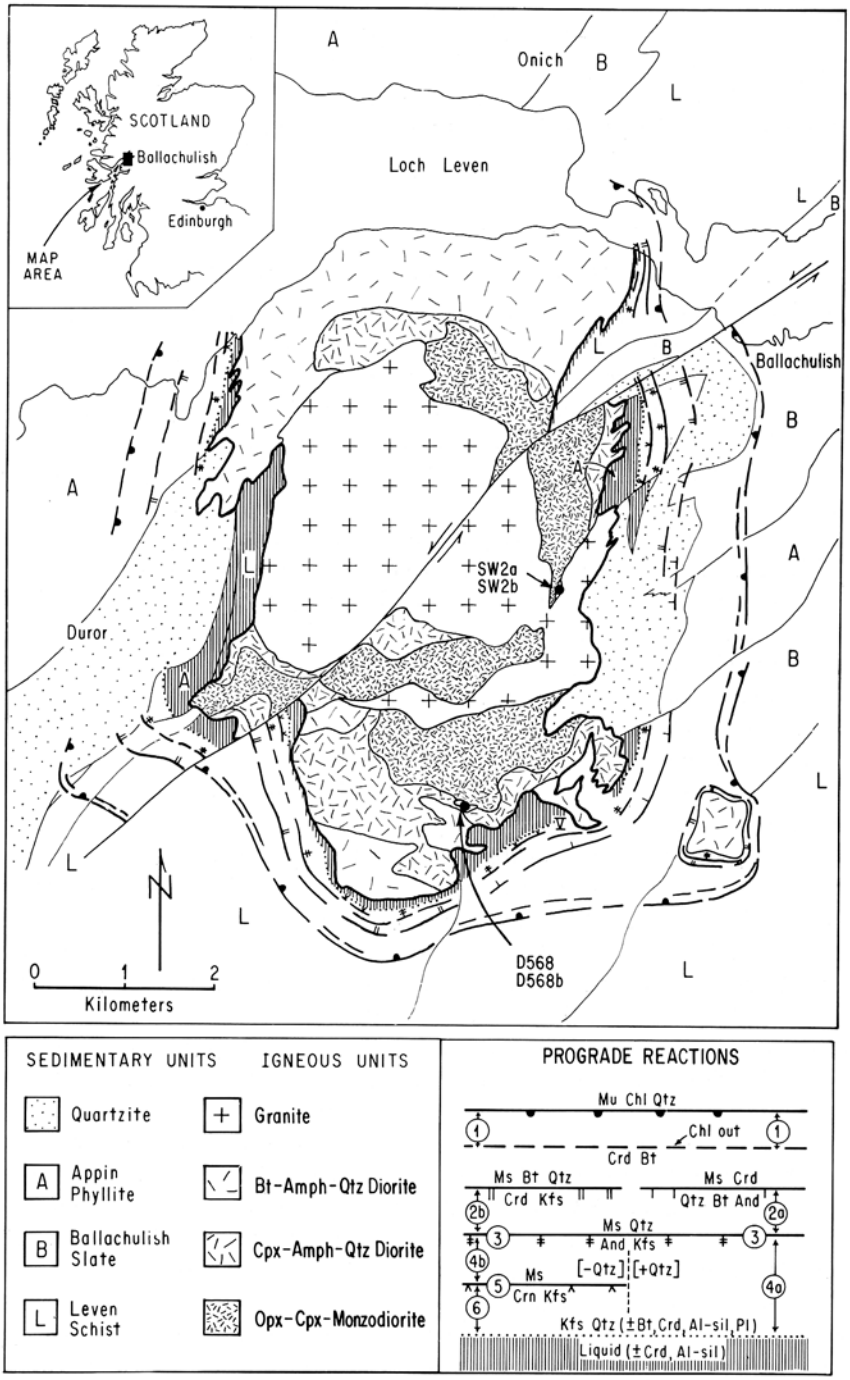

FIG. 1. Simplified geology of the Ballachulish Igneous Complex and contact aureole, showing the prograde reaction sequence and the location of specimens discussed in the text. For clarity, only major quartzite units and the three main pelitic units have been illustrated. A more complete stratigraphy is found in Bailey & Maufe (1960) and Pattison & Harte (1985). The geology of the igneous complex is from Weiss (1986, 1989) and the contact aureole from Pattison & Harte (1985).

enough for vapour-saturated melting to occur (see below and Pattison & Harte, 1988). Furthermore, there is only minor oxygen isotopic shift at the margins of the igneous complex, indicating a lack of exchange with an external fluid reservoir (Hoernes *et al.*, in press). Locally, there is stable isotope evidence for late exchange of magmatic fluids with marginal pelitic rocks up to a few hundred meters from the contact (Hoernes *et al.*, in press).

DERIVATION OF A QUANTITATIVE PETROGENETIC GRID

In this section, an attempt is made to derive a simple internally consistent thermodynamic data set to model the P–T positions of the reactions from the schematic grid in Fig. 2. The minerals included in the data set are listed in Table 1. Four internally consistent data sets have already been published that include cordierite: Helgeson *et al.* (1978), Droop & Treloar (1981), Berman (1988) and Spear & Cheney (1989). However, the predicted positions of some of the reactions (e.g. 2a and 2b), using each of these data sets, produces unacceptably large discrepancies in either slope or position from the experimentally determined reaction positions, and from constraints from natural assemblages (see below). It was therefore decided to derive a data set that provides a better fit to the available experimental data for the reactions in Table 2; consequently, it is much narrower in scope and less sophisticated in approach than some of the above larger data sets.

The theoretical approach used to derive the thermodynamic data is that of Fisher & Zen (1971), and is only briefly described here. The expression for chemical equilibrium between a

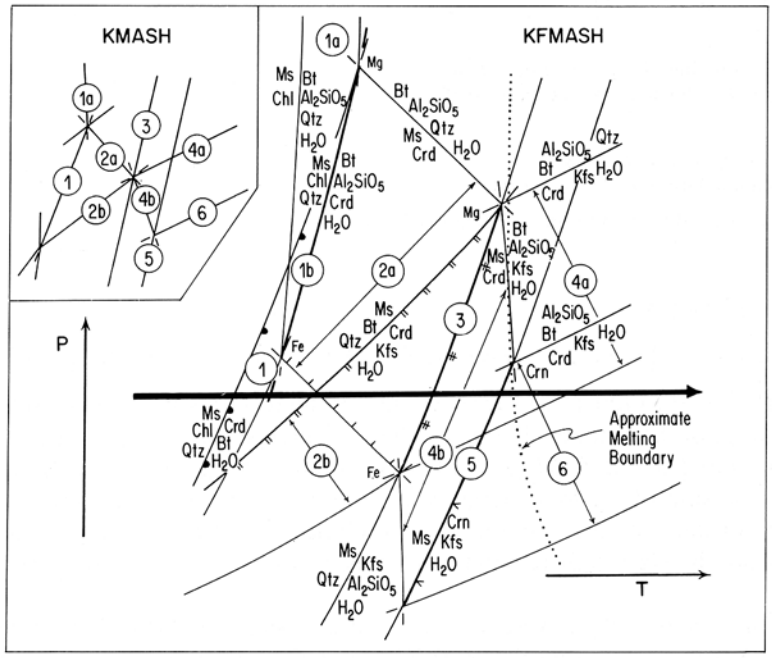

FIG. 2. Schematic petrogenetic grid in KFMASH showing the relationships between the different mineral reactions in Fig. 1. Ornaments on the reactions are the same as in Fig. 1. For simplicity, the divariant reactions are labelled on the bounding Mg end member curves, except for reaction 1a which is labelled on the Fe end member curve. For easier visualization of the topological relationships between the different reactions, the diagram in the upper left-hand corner is for either of the end member KMASH or KFASH systems.

TABLE 1

Phases and thermodynamic data

Phase	*Abbreviation*	*Formula*	H°_f *kJ*	S° kJ/Kelvin $\times 10^{-3}$	V° *kJ/kb*
Steam	H_2O	H_2O	−241·82	188·72	0·0
Quartz	Qtz	SiO_2	−910·65	41·34	2·269
Corundum	Crn	Al_2O_3	−1679·73	50·96	2·558
Andalusite	And	Al_2SiO_5	−2593·05	93·22	5·153
Kyanite	Ky	Al_2SiO_5	−2597·53	83·22	4·409
Sillimanite	Sil	Al_2SiO_5	−2589·90	96·11	4·990
Muscovite	Ms	$KAl_3Si_3O_{10}(OH)_2$	−5987·72	305·43	14·071
K-feldspar	Kfs	$KAlSi_3O_8$	−3969·57	228·70	10·905
Phlogopite	Phl	$KMg_3AlSi_3O_{10}(OH)_2$	−6230·81	319·24	14·991
Annite	Ann	$KFe_3AlSi_3O_{10}(OH)_2$	−5209·71	384·93	15·432
Mg-cordierite	Mg-Crd	$Mg_2Al_4Si_5O_{18}\cdot 0{\cdot}5H_2O$	−9352·04	410·03	23·772
Fe-cordierite	Fe-Crd	$Fe_2Al_4Si_5O_{18}\cdot 0{\cdot}5H_2O$	−8660·65	452·21	23·608
Clinochlore	Cch	$Mg_5Al_2Si_3O_{10}(OH)_8$	−8918·61	435·18	20·754

Sources for thermodynamic data

Volume

Quartz, corundum, andalusite, kyanite, sillimanite, muscovite, K-feldspar, phlogopite: Robie *et al.* (1978)
Annite: Helgeson *et al.* (1978)
Mg-cordierite: Droop & Treloar (1981)—average of anhydrous and hydrous Mg-cordierite of Helgeson *et al.* (1978)
Fe-cordierite: Droop & Treloar (1981)—anhydrous Fe-cordierite of Robie *et al.* (1978) plus half the difference of anhydrous and hydrous Mg-cordierite of Helgeson *et al.* (1978)
Clinochlore: Evans & Powell (1983)

Entropy

Steam, quartz, corundum: Helgeson *et al.* (1978)
Andalusite, kyanite, sillimanite: Robie *et al.* (1978)

Enthalpy

Steam, quartz: Helgeson *et al.* (1978)
Kyanite, sillimanite: Droop & Treloar (1981)

All other values derived from experimental data (see Table 2).

collection of phases is

$$\Delta G(P, T)=0=\Delta H^\circ(1, T)-T\Delta S^\circ(1, T)+P\Delta V^\circ_{sol}(P, T)+\Sigma RT\ln f_i+RT\ln K_{eq} \quad (1)$$

where $\Delta G(P, T)$ is the Gibbs free energy change of the reaction at P and T, $\Delta H^\circ(1, T)$ is the enthalpy change of the reaction at 1 b and the T of interest, $\Delta S^\circ(1, T)$ is the entropy change of the reaction at 1 b and T, $\Delta V^\circ_{sol}(P, T)$ is the volume change of the reaction at P and T, $\Sigma RT\ln f_i$ is the sum of the free energy contributions from fluid fugacities, and K_{eq} is the equilibrium constant for the reaction at a standard state of P and T. Fluid fugacities are calculated from the Hard Sphere Modified Redlich–Kwong equations of Kerrick & Jacobs (1981).

The thermodynamic data were derived using a stepwise fitting procedure, such as described in Appendix A of Powell (1978). The main differences in this study from Droop & Treloar (1981) are a more explicit correction for non-end member mineral compositions used in the experiments (see below), and the use of different fugacity equations. The Droop & Treloar data were used as a starting point, and modified on a trial and error basis until the calculated curves satisfied the majority of the experimental brackets.

TABLE 2

Summary of reaction stoichiometries and references to experimental data

Reaction no.	*Reaction*	*Reference*
1 (Mg)	Ms + Cch + 2 Qtz = Mg-Crd + Phl + 3·5 H_2O	1
1 (Fe)	Ms + Fe-Cch + 2 Qtz = Fe-Crd + Ann + 3·5 H_2O	—
1a (Mg)	5 Ms + 3 Cch = 5 Phl + 8 Al_2SiO_5 + Qtz + 12 H_2O	2
1a (Fe)	5 Ms + 3 Fe-Cch = 5 Ann + 8 Al_2SiO_5 + Qtz + 12 H_2O	—
1b (Fe, Mg)*	Ms + Chl + Qtz = Crd + Bt + Al_2SiO_5 + H_2O	—
2a (Mg)	2 Ms + 3 Mg-Crd = 2 Phl + 8 Al_2SiO_5 + 7 Qtz + 1·5 H_2O	1, 2
2a (Fe)	2 Ms + 3 Fe-Crd = 2 Ann + 8 Al_2SiO_5 + 7 Qtz + 1·5 H_2O	—
2b (Mg)	6 Ms + 2 Phl + 15 Qtz = 3 Mg-Crd + 8 Kfs + 6·5 H_2O	3
2b (Fe)	6 Ms + 2 Ann + 15 Qtz = 3 Fe-Crd + 8 Kfs + 6·5 H_2O	—
3	Ms + Qtz = Kfs + Al_2SiO_5 + H_2O	4
4a (Mg)	2 Phl + 6 Al_2SiO_5 + 9 Qtz = 3 Mg-Crd + 2 Kfs + 0·5 H_2O	5
4a (Fe)	2 Ann + 6 Al_2SiO_5 + 9 Qtz = 3 Fe-Crd + 2 Kfs + 0·5 H_2O	5
4b (Mg)	9 Ms + 3 Mg-Crd = 2 Phl + 15 Al_2SiO_5 + 7 Kfs + 8·5 H_2O	—
4b (Fe)	9 Ms + 3 Fe-Crd = 2 Ann + 15 Al_2SiO_5 + 7 Kfs + 8·5 H_2O	—
5	Ms = Crn + Kfs + H_2O	4
6 (Mg)	2 Phl + 15 Al_2SiO_5 = 3 Mg-Crd + 9 Crn + 2 Kfs + 0·5 H_2O	—
6 (Fe)	2 Ann + 15 Al_2SiO_5 = 3 Fe-Crd + 9 Crn + 2 Kfs + 0·5 H_2O	—
—	And = Sil	6, 7
—	Ky = Sil	6, 7
—	Ky = And	6, 7

* Reaction stoichiometry depends on Mg/(Mg + Fe) in minerals.

1—Seifert (1970). 2—Bird & Fawcett (1973). 3—Seifert (1976). 4—Chatterjee & Johannes (1974). 5—Holdaway & Lee (1977). 6—Holdaway (1971). 7—Richardson *et al.* (1969).

The data derived for each mineral are H_f°, S° and V°, all for the P–T range of the experiments. The simplifying assumptions have been made that the net change in the heat capacity for the reactions is zero (i.e., $\Delta C_p = 0$), and that change in isothermal compressibility and thermal expansion of the minerals is also zero. The $\Delta C_p = 0$ simplification is in contrast to some of the above data sets which incorporate expressions for the variation of C_p with T for each mineral. This simplified approach is adopted because it is possible over the P–T range of interest to model adequately the experimentally determined reaction positions without incorporating the ΔC_p expressions, and, more importantly, the error introduced by neglecting to incorporate these expressions is minor compared with that of some of the other major assumptions that have to be made to derive the data (see below). In view of this, the thermodynamic data listed in Table 1 may be different from those derived from calorimetry and more rigorously modelled phase equilibria, and should therefore not be used as reliable primary thermodynamic data.

Difficulties in deriving thermodynamic data

Examining eqn. (1), it is necessary to know, in addition to the enthalpies, entropies, and volumes of the minerals, the compositions of all of the minerals, because of the $RT \ln K$ term. Even in the simplified KFASH or KMASH systems, chlorite, muscovite, and biotite undergo Tschermak exchange ((Fe, Mg)Si = 2Al), and cordierite has a variable water content. Both the Tschermak exchange and cordierite water content vary with P and T. If the compositions of all the phases in the experiments are not known, then it is necessary to estimate their compositions.

Cordierite and its water content

The experiments of Schreyer & Yoder (1964) and Mirwald & Schreyer (1977) showed that the water content of Mg-cordierite varies with P and T. However, in the experiments of Seifert (1970), Bird & Fawcett (1973), Seifert (1976) and Holdaway & Lee (1977), the H_2O content of cordierite was not measured in the runs (see Lonker, 1981, for a discussion of the difficulties of measuring cordierite H_2O contents from experimental runs). In the approximate range of P–T conditions in which cordierite-bearing reactions typically occur in contact metamorphism (2–4 kb, 500–700 °C), the H_2O content of cordierite is 1·3–1·6 wt.%, or 0·4–0·55 mol (see fig. 2 of Newton & Wood, 1979). Thus, the simplifying assumption has been made that cordierite contains 0·5 moles of structurally bound water (see also Droop & Treloar (1981) and Bird & Fawcett (1973), who made the same assumption). This treatment of cordierite water content is in contrast to that of Newton & Wood (1979), who calculated $G_f^\circ(1, 298)$ values for Mg-cordierite for different degrees of cordierite hydration. However, incorporation of their P–T–H_2O dependent H_2O values did not improve the fit of the calculated reaction positions with the experiments, so that for simplicity, this refinement was omitted.

(Fe, Mg)Si = 2Al in chlorite, muscovite, and biotite

Chlorite, muscovite, and biotite rarely, if ever, occur in nature as the end member phases clinochlore $Mg_5Al_2\ Si_3O_{10}(OH)_8$, muscovite *sensu stricto* $KAl_3Si_3O_{10}(OH)_2$, and phlogopite $KMg_3AlSi_3O_{10}(OH)_2$, even though thermodynamic properties are usually calculated for these end members. In the experimental studies of Seifert (1970, 1976), Bird & Fawcett (1973), and Holdaway & Lee (1977) on reactions 1, 1a, 2a, 2b, and 4a, the compositions of chlorite, muscovite, and phlogopite before and after the runs were not measured. Seifert (1976) noted from X-ray diffraction analysis that the compositions of Mg-biotite changed during the runs from phlogopite (inserted) to a more eastonitic composition, but he was unable to determine quantitatively the change.

One way to estimate the compositions of chlorite, muscovite, and biotite in the experiments is to model them on natural mineral compositions in rocks containing the same assemblages as the experiments. The activity of the end members may then be calculated from an appropriate activity–composition model. Activity–composition models for micas are still somewhat controversial, so for simplicity the ideal mixing-on-sites model has been adopted (see Table 3 for a complete list of activity–composition expressions for all phases in the study).

Holdaway & Lee (1977), in their experiments on reaction 4a, provided a best estimate composition of their biotites of $K_{0·84}(Fe, Mg)_{2·52}Al_{1·72}Si_{2·74}O_{10}(OH)_2$, based on natural biotites from Guidotti *et al.* (1975). From this composition, the activity of annite and phlogopite is calculated to be $a_{Ann} = a_{Phl} = 0·48$, assuming either pure Fe or Mg (Table 4). If the biotite were assumed to be end member annite or phlogopite, significant error would result in the derived thermodynamic data for these end members.

Holdaway & Lee's (1977) biotite composition and calculated activity of 0·48 have been used for reactions 2b and 4a in this study. For reactions 1 and 1a, biotite is more enriched in the phlogopite–annite end member than in reactions 2b and 4a (Pattison, 1987); an appropriate average composition is $(K + Na)_{0·8}(Mg, Fe)_{2·6}Al_{1·6}Si_{2·8}O_{10}(OH)_2$, resulting in an activity of phlogopite (assuming pure K and Mg) of 0·51.

Natural muscovite in and upgrade of reaction 2b has an average composition of $(K + Na)_{0·90}(Mg, Fe)_{0·2}Al_{2·7}Si_{3·1}O_{10}(OH)_2$, giving an activity of 0·72 (assuming $K = 0·90$ in the Na-absent experiments). Muscovite in reaction 1 has a typical composition of

$(K+Na)_{0.85}(Mg, Fe)_{0.28}Al_{2.6}Si_{3.2}O_{10}(OH)_2$, giving an activity of 0·67 (assuming K = 0·85). Natural chlorite from reaction 1 has an average composition of $(Mg, Fe)_{4.65}Al_{2.7}Si_{2.65}O_{10}(OH)_8$, giving an activity of clinochlore of 0·86 (assuming pure Mg).

Although it is recognized that the compositions of natural sheet silicates vary smoothly with P and T, the above estimates are a first-order correction for the non-end member compositions of the minerals in the experimental runs. The effect of the non-end member compositions of chlorite, muscovite, and biotite tend to be cancelling in reactions 1, 1a, 2a, and 4b, because they are arranged on opposite sides of the reaction. However, in reactions 2b and 4a, the effect of non-end member compositions is significant.

Comparison of calculated vs experimental reaction positions

The exact reaction stoichiometries, assumed mineral compositions and calculated activities are listed in Tables 3 and 4. The derived thermodynamic data for the end members are listed in Table 1. In the subsystem KASH, the calculated positions of the reactions $Ms + Qtz = And + Kfs + H_2O$, $Ms + Qtz = Sil + Kfs + H_2O$, and $Ms = Crn + Kfs + H_2O$ satisfy all of the experimental brackets of Chatterjee & Johannes (1974).

Figure 3 illustrates the positions of the calculated curves and the experimental brackets in the full KFMASH system. Overall, the fit is good, with the main exception of reaction 2a ($Ms + Crd = Al_2SiO_5 + Bt + Qtz + H_2O$). In Fig. 3, reaction 2a emanating from the KMASH invariant point (Crn, Kfs) (terminology as in Pattison & Harte, 1985) does not coincide with reaction 2a emanating from KMASH invariant point (Crn, Chl), because the activities of Ms, Bt, and Chl at the two invariant points are assumed to be different (see above discussion and Table 3).

The calculated slope of reaction 2a, with sillimanite or andalusite as the Al_2SiO_5 polymorph, is subhorizontal to slightly negative, compared with the steeper negative slope required by the experimental brackets of Seifert (1970) and Bird & Fawcett (1973) (represented by the dotted line in Fig. 4). Additional evidence for a negative slope for reaction 2a is provided by the experiments of Hirschberg & Winkler (1968), in which Bt and Crd in the

TABLE 3

Mineral activity–composition formulations (ideal mixing-on-sites model)

Mineral	*End member*	*Formula*	*Activity formulation*
Chlorite	Clinochlore	$Mg_5Al_2Si_3O_{10}(OH)_8$	$a^{Chl}_{Cch} = 64\,(X^{Brc}_{Mg})^2(X^{Brc}_{Al})(X^{Tlc}_{Mg})^3(X^{IV}_{Al})(X^{IV}_{Si})^3$ where $X^{Brc}_{Al} = Al^{VI}$
White mica	Muscovite	$KAl_3Si_3O_{10}(OH)_2$	$a^{WM}_{Ms} = 9{\cdot}48\,(X^{A}_{K})(X^{M2}_{Al})^2(X^{M1}_{\square})(X^{IV}_{Al})(X^{IV}_{Si})^3$
Biotite	Annite	$KFe_3AlSi_3O_{10}(OH)_2$	$a^{Bt}_{Ann} = 9{\cdot}48\,(X^{A}_{K})(X^{M2}_{Fe})^2(X^{M1}_{Fe})(X^{IV}_{Al})(X^{IV}_{Si})^3$
	Phlogopite	$KMg_3Al_3O_{10}(OH)_2$	$a^{Bt}_{Phl} = 9{\cdot}48\,(X^{A}_{K})(X^{M2}_{Mg})^2(X^{M1}_{Mg})(X^{IV}_{Al})(X^{IV}_{Si})^3$
Cordierite	Fe-cordierite	$Fe_2Al_4Si_5O_{18}{\cdot}0{\cdot}5H_2O$	$a^{Crd}_{Mg\text{-}Crd} = (X_{Fe})^2$
	Mg-cordierite	$Mg_2Al_4Si_5O_{18}{\cdot}0{\cdot}5H_2O$	$a^{Crd}_{Mg\text{-}Crd} = (X_{Mg})^2$
Alkali-feldspar	K-feldspar	$KAlSi_3O_8$	$a^{AF}_{Kfs} = X^{A}_{K}$
Orthopyroxene	Ferrosillite	$Fe_2Si_2O_6$	$a^{Opx}_{Fs} = (X^{M2}_{Fe})(X^{M1}_{Fe})$
	Enstatite	$Mg_2Si_2O_6$	$a^{Opx}_{En} = (X^{M2}_{Mg})(X^{M1}_{Mg})$
Pleonaste-spinel	Hercynite	$FeAl_2O_4$	$a^{Pleon}_{Hc} = (X^{M}_{Fe})(X_{Al})^2$
	Spinel	$MgAl_2O_4$	$a^{Pleon}_{Spl} = (X^{M}_{Mg})(X_{Al})^2$

Activity formulation for chlorite from Graham *et al.* (1983); all other minerals from Powell (1978).

TABLE 4

Mineral compositions and calculated activities used in the derivation of the thermodynamic data (Column 1) and in the calculation of Fig. 4 (Column 2)

Reaction no.	*Mineral*	*(1) Derivation of thermodynamic data*	*(2) Calculation of Fig. 4*
1, 1a	Ms	$K_{0.85}(Fe, Mg)_{0.3}Al_{2.6}Si_{3.2}O_{10}(OH)_2$ $a_{Ms}^{WM}=0.67$	$(K_{0.75}Na_{0.10})(Fe, Mg)_{0.3}Al_{2.6}Si_{3.2}O_{10}(OH)_2$ $a_{Ms}^{WM}=0.59$
	Chl	$(Mg, Fe)_{4.65}Al_{2.7}Si_{2.65}O_{10}(OH)_8$ $a_{Cch}^{Chl}=0.86$	$(Mg, Fe)_{4.6}Al_{2.73}Si_{2.65}O_{10}(OH)_8$ $a_{Cch}^{Chl}=0.82$
	Bt	$K_{0.8}(Fe, Mg)_{2.6}Al_{1.6}Si_{2.8}O_{10}(OH)_2$ a_{Phl}^{Bt}, $a_{Ann}^{Bt}=0.51$	$K_{0.80}(Fe, Mg)_{2.45}Al_{1.75}Ti_{0.06}Si_{2.7}O_{10}(OH)_2$ a_{Phl}^{Bt}, $a_{Ann}^{Bt}=0.41$
2a, 2b, 4a, 4b, 6	Ms	$K_{0.90}(Fe, Mg)_{0.2}Al_{2.7}Si_{3.1}O_{10}(OH)_2$ $a_{Ms}^{WM}=0.72$	$(K_{0.85}Na_{0.05})(Fe, Mg)_{0.2}Al_{2.7}Si_{3.1}O_{10}(OH)_2$ $a_{Ms}^{WM}=0.68$
	Bt	$K_{0.84}(Fe, Mg)_{2.52}Al_{1.72}Si_{2.74}O_{10}(OH)_2$ a_{Phl}^{Bt}, $a_{Ann}^{Bt}=0.48$	$K_{0.9}(Fe, Mg)_{2.35}Al_{1.75}Ti_{0.14}Si_{2.65}O_{10}(OH)_2$ a_{Phl}^{Bt}, $a_{Ann}^{Bt}=0.40$
	Kfs	$KAlSi_3O_8$ $A_{Kfs}^{AF}=1.0$	$(K_{0.8}Na_{0.2})AlSi_3O_8$ $a_{Kfs}^{AF}=0.80$
3, 5	Ms	$KAl_3Si_3O_{10}(OH)_2$ $a_{Ms}^{WM}=1.0$	$(K_{0.85}Na_{0.05})(Fe, Mg)_{0.2}Al_{2.7}Si_{3.1}O_{10}(OH)_2$ $a_{Ms}^{WM}=0.68$
	Kfs	$KAlSi_3O_8$ $A_{Kfs}^{AF}=1.0$	$(K_{0.8}Na_{0.2})AlSi_3O_8$ $a_{Kfs}^{AF}=0.80$

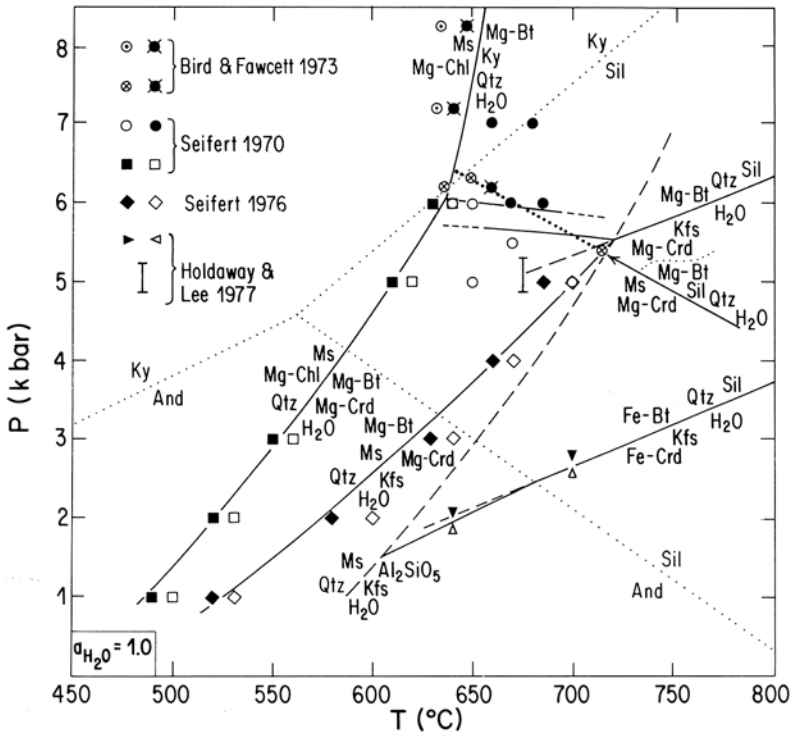

FIG. 3. Comparison of calculated curves with experimental data in KFMASH, using the thermodynamic data, reaction stoichiometries and activities in Tables 1, 2, and 4. For reaction 2a, Ms + Mg-Crd = Mg-Bt + Qtz + Sil + H_2O, the data points of both Seifert (1970) and Bird & Fawcett (1973) are included; the filled symbols with or without crosses are for Bt + Qtz + Sil stable, the open circles with or without crosses are for Ms + Crd stable. The calculated positions of reaction 2a do not join up because different mineral activities were used for reactions 1 and 1a from those for reactions 2a, 2b, and 4a (see text and Table 4). A best-fit line that satisfies the brackets has been dotted in. The 675 °C vertical bracket from Holdaway & Lee (1977) is for the reaction Mg-Bt + Sil + Qtz = Mg-Crd + Kfs + H_2O. Reaction 3, Ms + Qtz = Al_2SiO_5 + Kfs + H_2O, has been calculated for $a_{Ms} = 0{\cdot}85$, to be consistent with the a_{Ms} for the other curves.

assemblage Ms + Qtz + Bt + Crd + Al_2SiO_5 became more Mg-rich with isobaric increase in temperature (see Fig. 2), and the isobaric prograde path in the Ballachulish aureole, in which andalusite is developed in the assemblage Ms + Qtz + Crd + Bt + Al_2SiO_5 upgrade along strike of the assemblage Ms + Qtz + Crd + Bt (see Figs. 1 and 2).

The experimental brackets for all of the other reactions are satisfied to within 5 °C, with the exception of the 3 kb bracket for reaction 2b, whose position is 10 °C above the calculated curve. Although the experiments of Holdaway & Lee (1977) did not constrain the slope of reaction 4a in the pure Mg system, the slope in Fig. 4 is consistent with Hoffer's (1976) experiments on this reaction for intermediate compositions, and is subparallel to the reaction in the pure Fe system.

Overall, it appears that the experimental data are not internally consistent—no amount of thermodynamic massaging could produce a calculated set of curves that satisfied all of the experimental brackets. Although some of the problem no doubt lies with the simplified treatment of the P–T dependence of mineral compositions, it is likely that further reversed experiments, with attention paid to the compositions of all of the phases, will be required before the internal consistency problems in this system can be cleared up.

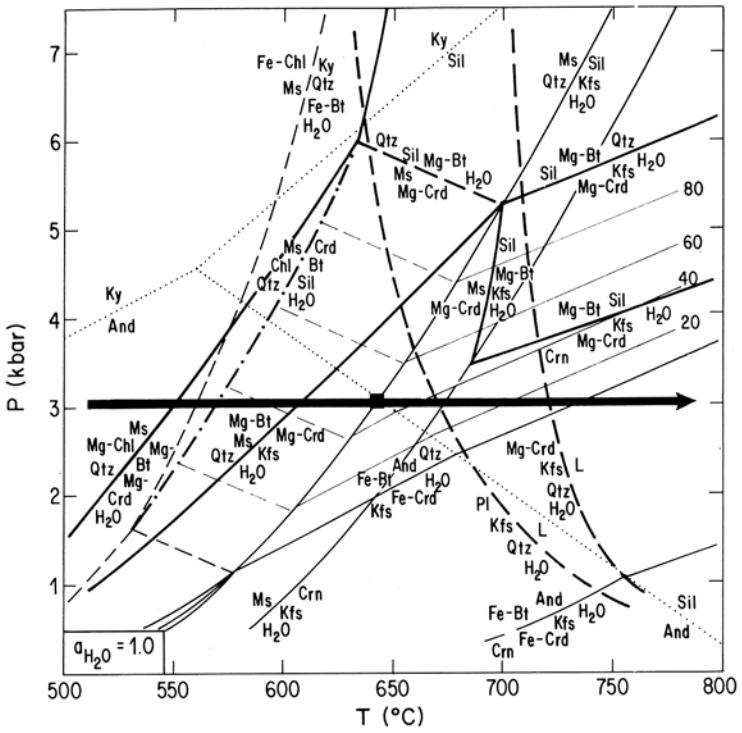

FIG. 4. Calibrated petrogenetic grid for typical pelitic mineral compositions in the Ballachulish and other contact aureoles (see Table 4 for mineral compositions and activities). Heavy lines are for KMASH bounding curves, light lines are for KFASH bounding curves, and the dot–dash line is for the KFMASH univariant reaction $Ms + Chl + Qtz = Al_2SiO_5 + Crd + Bt + H_2O$. Solid lines are curves calculated from the data of Tables 1, 2, and 4. The dashed lines are the estimated positions of reactions, as discussed in the text. The melting reactions $An_{30} + Kfs + Qtz + H_2O = L$ and $Mg\text{-}Crd + Kfs + Qtz + H_2O = L$ are from Thompson & Tracy (1979) and Seifert (1976), respectively. Isopleths of Mg/(Mg + Fe) in cordierite have been drawn through KFMASH divariant reactions 2a and 4a according to Holdaway & Lee (1977). The solid horizontal line is drawn for the 3 kb isobaric trajectory in the aureole (see text for the calculation of this pressure).

The data set in Table 1 is that which best reproduced the experimental data for reactions 1, 2b, and 4a, because these reactions form the most important mineral assemblage boundaries in the Ballachulish and several other contact aureoles.

A petrogenetic grid for contact metamorphic pelites

Using the thermodynamic data set described above, Fe and Mg end member reactions in Table 2 were calculated and plotted in Fig. 4. Figure 4 has been calculated for typical natural mineral compositions measured in the Ballachulish aureole (Pattison, 1987). The model mineral compositions and activities are listed in Table 4. K/(K + Na) ratios for muscovite and K-feldspar are assumed to be 0·95 and 0·8, respectively. Activity of water for all subsolidus reactions is assumed to be unity. Figure 5 shows more clearly the most common range of cordierite Mg/(Mg + Fe) ratios (0·45–0·65) in the Ballachulish and other thermal aureoles, in addition to some high-grade reactions discussed below. Assuming that pelites in the Ballachulish aureole are of 'normal' composition, Figs. 4 and 5 are applicable to contact metamorphosed pelites in general.

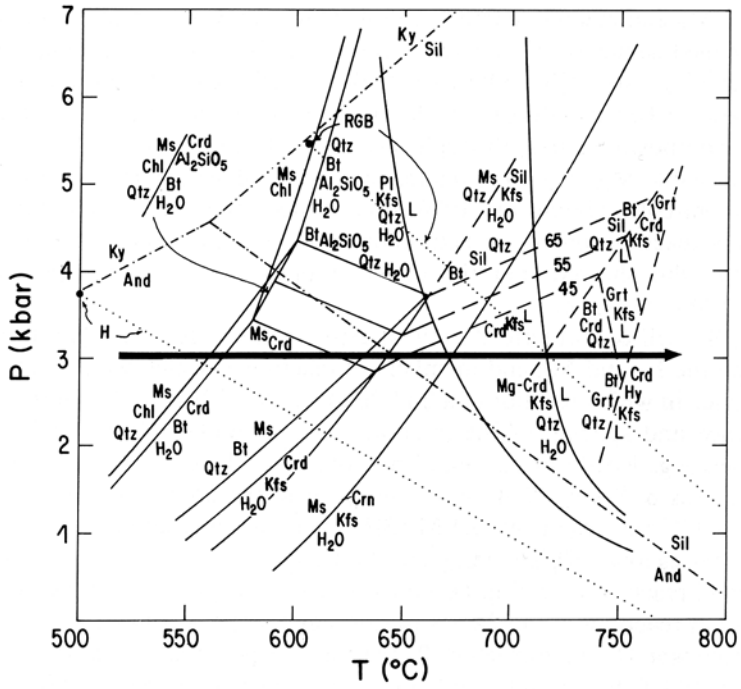

FIG. 5. Abstracted portion of Fig. 4 for the most common range of Mg/(Mg + Fe) in cordierite in the Ballachulish and other contact aureoles (0·45–0·65). Also included are the estimated positions of high-grade reactions that produce garnet and hypersthene (Grant, 1985, and other references in the text). Isopleths of Mg/(Mg + Fe) in cordierite have been extended into the higher-grade divariant reactions. The dotted lines labelled H and RGB are the And = Sil boundaries of Holdaway (1971) and Richardson *et al.* (1969). The solid dots at the end of each boundary are the respective authors' triple points. Activity of water is assumed to be 1·0 below the vapour saturated solidi; above the solidi, it is assumed to be internally buffered below 1·0. The solid line is the 3 kb isobaric trajectory at Ballachulish.

Because of the difficulties in calculating the slope and position of reaction 2a to satisfy the experimental data, it has simply been drawn to connect the two calculated invariant points (Crn, Chl) and (Crn, Kfs) in Fig. 4. The resulting slope is parallel to that required by the experimental data of Seifert (1970) and Bird & Fawcett (1973). Fe–Mg divariant reaction 4a has been contoured with isopleths of Mg/(Mg + Fe) in cordierite, calculated using the data of Holdaway & Lee (1977). These isopleths have been correspondingly extended into divariant reaction 2a.

Included in Figs. 4 and 5 are two vapour-saturated melting reactions. The lower-temperature reaction is $An_{30} + Kfs + Qtz + H_2O = L$, interpolated from the positions of the Ca and Na end member reactions of Thompson & Tracy (1979). The higher-temperature reaction is Mg-Crd + Kfs + Qtz + H_2O = L, from Seifert (1976). These are representative of the most important vapour-saturated melting reactions in the aureole (Pattison & Harte, 1988). The position of the lower melting curve satisfies the observation that anatectic migmatization commences in the field near the reaction Ms = Cor + Kfs + H_2O (see Fig. 1).

Reaction 1, Ms + Chl + Qtz = Crd + Bt + H_2O

In the absence of experimental data on the reactions involving Fe-chlorite, the Fe-analogue of reaction 1, Fe-Chl + Ms + Qtz = Fe-Crd + Fe-Bt + H_2O, has been located 25 °C

higher than the Mg end member curve in Fig. 4. This narrow temperature interval is based on the well-defined sequence of mineral zones in the Ballachulish aureole, in which the reaction 1 assemblage Ms + Chl + Qtz + Crd + Bt is restricted on the ground to a consistent but very narrow (< 100 m) interval on the outer edge of the aureole. A broad range of Mg/(Mg + Fe) compositions pass through this reaction (see Fig. 3a of Pattison, 1987), but there is no noticeable Mg/(Mg + Fe)-related shift in the development of cordierite by this reaction in the aureole. Thompson (1976) also argued for a narrow (20 °C) temperature interval for this reaction, based on field constraints and the experiments of Fleming & Fawcett (1976), who showed that the upper stability limit of Chl + Qtz is essentially independent of Mg/(Mg + Fe).

In contrast, Burnell & Rutherford's (1984) experiments suggest a separation of at least 150 °C between the Fe and Mg end members of reaction 1, which would fully occupy the part of P–T space in which reactions 2a and 2b are stable. This would contradict the well-defined sequence and spacing of the mineral zones at Ballachulish and in many other thermal aureoles (e.g., Rove Formation, Minnesota, Labotka *et al.*, 1981; Lilesville aureole, N. Carolina, Evans & Speer, 1984). Assuming instead the 25 °C separation, reaction 1 is effectively (±5 °C) univariant in KFMASH over the measured range of cordierite Mg/(Mg + Fe) ratios (0·4–0·7), assuming constant a_{H_2O}.

The position of reaction 1b in Fig. 4 is constrained by the positions of the Fe and Mg end member curves of reactions 1 and 2a. Its position and slope is comparable to that of Hess (1969) and Thompson (1976). Burnell & Rutherford's experiments suggest that reaction 1b is located about 100 °C higher in the low pressure range 2–4 kb; this must be cast in doubt, because there is no evidence for the operation of this reaction in the aureole and the stability fields of reactions 2a and 2b would be eliminated.

Andalusite–sillimanite

In Fig. 5 the And = Sil reaction has been located between the Richardson *et al.* (1969) and Holdaway (1971) determinations, similar to that calculated by Droop & Treloar (1981) and Holland & Powell (1985). The location of the And = Sil transition is consistent with the first appearance of sillimanite at the Ms + Qtz breakdown, assuming a pressure of 3 kb (see below).

Andalusite is the only polymorph present downgrade of reaction 3 (Ms + Qtz = Al_2SiO_5 + Kfs + H_2O). Sillimanite first occurs in assemblages at reaction 3 in 0·5–2 mm-long prisms in cordierite, and in fibrous sprays surrounding accessory minerals. The thickness of the sillimanite prisms normal to the c-axis ranges between 5 and 50 μm, which overlaps the arbitrary 10 μm boundary used by Kerrick & Spear (1988) to distinguish between fibrolite and sillimanite. Volumetrically, however, >95% of the Al_2SiO_5 is andalusite, which appears to be the polymorph in textural equilibrium with the other minerals in the rock, occurring in spongy poikiloblasts intergrown with K-feldspar and biotite in a granulose matrix of Kfs + Crd + Bt ± Qtz + Ilm. From reaction 3 upgrade, both polymorphs are found. Although sillimanite becomes more abundant and coarser as the igneous contact is approached, 90–95% of the Al_2SiO_5 is andalusite, and it continues to appear texturally to be the polymorph in equilibrium with the other minerals in the rocks (Pattison & Harte, in press).

In contrast to specimens from a number of contact aureoles described by Kerrick (1987), the association of fibrolitic sillimanite with biotite is not common at Ballachulish, and there is no correlation between the development of sillimanite and zones of alteration or late hydrothermal exchange (Pattison & Harte, in press). Rather, the gradual increase in grain

size and modal abundance of sillimanite suggests that it was formed during prograde contact metamorphism.

Fe_2O_3 contents of andalusite and sillimanite were measured in a number of rocks. Weight % Fe_2O_3 in sillimanite ranges from 0·21 to 1·12, and in andalusite from 0·14 to 0·33. The Fe_2O_3 contents of andalusite and sillimanite in one thin section (D25a) are 0·14 and 0·24 wt.%, respectively, giving a $K = a^{Sil}_{Al_2SiO_5}/a^{And}_{Al_2SiO_5} = 0{\cdot}998$ (see Kerrick & Speer, 1988). Moreover, in the large majority of Al_2SiO_5-bearing specimens, ilmenite is the only oxide phase present, so one would predict that the Fe^{3+} contents in the polymorphs would be relatively minor. In summary, a significant effect on the equilibrium due to partitioning of Fe^{3+} between the polymorphs (Kerrick & Speer, 1988) is not considered to be important.

Because of the somewhat ambiguous relationship between andalusite and sillimanite above reaction 3, it is obvious that their occurrence together is not very informative about equilibrium P–T conditions. However, accepting the first appearance of sillimanite as a significant, and mappable, prograde boundary, it seems clear that the Richardson *et al.* (1969) boundary is too high (see Fig. 5). The Holdaway (1971) boundary remains a possibility only if one argues for a kinetic delay in the growth of sillimanite of ~100 °C at 3 kb. It has been decided to use the curve in Fig. 5 as the best practical boundary between sillimanite-bearing and sillimanite-absent rocks, even though it is possible that this boundary may be particular to the sillimanite crystal size, degree of Al–Si disorder, minor element composition and rate of heating in the Ballachulish aureole.

Above the And–Sil boundary it is possible that reactions involved both polymorphs. For simplicity, reactions involving Al_2SiO_5 above this boundary have been calculated with sillimanite; using andalusite does not substantially affect the diagram.

PRESSURE AND TEMPERATURES IN THE BALLACHULISH AUREOLE

Using Fig. 4, pressure was estimated in the Ballachulish aureole. The Mg/(Mg + Fe) composition of cordierite in three specimens containing the model univariant assemblage Ms + Qtz + Bt + Crd + And(Sil) + Kfs is 0·50 (see detailed discussion in Pattison, 1987). The intersection of the 0·50 isopleth with reaction 3 gives a pressure of 3·1 kb. This is similar to the 2·9 kb estimate using fig. 7 of Holdaway & Lee (1977). Holdaway & Lee quoted the pooled uncertainty (e.g., cordierite water content, experimental precision) of pressure estimates obtained from the intersection of isopleths of reaction 4a with reaction 3 as ±0·4 kb. Adding a small amount of uncertainty for the difference in calculated activities between the natural minerals and the estimated mineral compositions used in the derivation of the thermodynamic data, a total uncertainty of ±0·5 kb is felt to be reasonable. Temperature uncertainty (same sources) for the best constrained reactions 1, 2a, 3, and 5 is estimated as ±20 °C; for reactions 2a, 4a, 4b, and 6, which have flatter P–T slopes, the uncertainty may be greater.

Using a pressure of 3 kb, a quantitative T–X_{Fe-Mg} diagram was calculated (Fig. 6). The Mg/(Mg + Fe) ratios of cordierite and biotite on reaction 3 were taken to be 0·50 and 0·38, respectively, based on the mineral data in Pattison (1987). This gives a $K = (Mg/Fe)Bt/(Mg/Fe)Crd = 0{\cdot}61$. There is no significant measured variation of K with grade in the aureole (Pattison, 1987; Fig. 4), so it has been assumed to be constant over the interval 550–700 °C.

From Figs. 5 and 6, temperatures may be assigned to the reaction boundaries in the aureole. These are listed in Table 5. For Fe–Mg continuous reactions, temperatures in Table 5 represent the lowest possible for the measured mineral compositions.

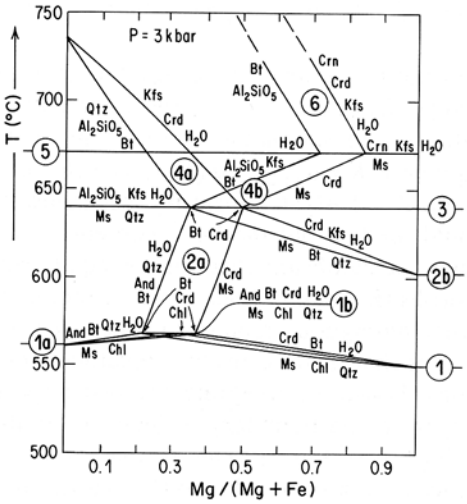

FIG. 6. Calculated 3 kb isobaric T–X_{Fe-Mg} diagram for the reactions in Figs. 2 and 5.

TABLE 5

Temperatures (°C) of major mineral assemblage boundaries in the Ballachulish aureole, for P = 3 kb. Uncertainties are discussed in the text

Non-graphitic pelites	*Prograde reaction*	*Graphitic pelites*
560	Ms Chl Qtz = Crd Bt H_2O	550
	Ms Crd = And Bt Qtz H_2O	600
620	Ms Bt Qtz = Crd Kfs H_2O	
640	Ms Qtz = Kfs Al_2SiO_5 H_2O	625
670	Ms = Crn Kfs H_2O	655
670	Kfs Pl Qtz H_2O = L	715
720	Kfs Crd Qtz H_2O = L	775
750	Bt Crd Qtz = Grt Kfs L	N/A
760	Bt Grt Qtz = Hy Crd Kfs L	N/A

HIGH-GRADE ASSEMBLAGES

Immediately adjacent to the igneous contacts and within coherent pelitic screens surrounded by the igneous complex, high-grade garnet + cordierite + biotite ± hypersthene assemblages are found in quartz-bearing rocks. These assemblages are suitable for the application of a number of calibrated geothermometers and geobarometers, to allow some estimation of temperature in the migmatitic zone and to obtain pressure estimates to compare with the 3 kb estimate from the petrogenetic grid. The samples analysed are located in Fig. 1. Table 6 lists the mineral compositions and calculated temperatures and pressures. All details of the different calibrations are listed at the bottom of the table.

Garnet was analysed from specimens found in two pelitic screens within the igneous complex (see Fig. 1). In the more northerly screen (SW2a and SW2b), it is present in the assemblage Grt + Bt + Crd + Qtz + Kfs + Pl + Ilm + (inferred melt), whilst in the more southerly screen (D567 and D568), it is present in the assemblage Grt + Bt + Crd ± Hy + Qtz + Pl + Ilm + (inferred melt).

The garnet occurs as 1–3 mm euhedral, unaltered crystals, and contains inclusions of quartz, ilmenite, biotite, and altered cordierite. The garnet chemical data in Table 6 are from the cores of flat compositional plateaux away from any inclusions. At the rims of garnets in SW2a and SW2b, there is an increase in X_{Mn} from 0·05 to 0·09 and a decrease in X_{Mg} from 0·14 to 0·09, with Fe and Ca remaining constant; this is suggestive of garnet resorption (Tracy, 1982). At the rims of garnets in D567 and D568, in contrast, Ca and Mn remain constant, whilst X_{Fe} increases from 0·76–0·78 to 0·79–0·83 and X_{Mg} decreases from 0·16–0·17 to 0·10–0·14. The difference in Mg/(Mg + Fe) between the rims and cores is dependent upon the minerals adjacent to the garnet (e.g., there is negligible variation beside quartz and maximal variation beside biotite), which suggests diffusive re-equilibration rather than resorption. In both cases, apparent temperatures are lower by 100–150 °C using rim compositions.

Cordierite occurs both as discrete prismatic crystals (1–2 mm) and in polycrystalline aggregates, with no consistent variation in Mg/(Mg + Fe) from core to rim. The hypersthene in D568 is present as 0·5–2 mm euhedral, strongly pleochroic crystals containing inclusions of quartz. There is no apparent core–rim zonation in Mg/(Mg + Fe). Al_2O_3 content is 2·6 wt.%.

Biotite in SW2a and SW2b occurs as 0·2–1 mm discrete tabular crystals. In contrast, in D567 and D568, the biotite occurs as 2–4 mm poikiloblastic crystals that overgrow quartz, hypersthene, garnet, and plagioclase. This texture suggests that the biotite may be of a late origin. In both cases, there is no significant compositional zoning.

High-grade reactions

The model KFMASH reactions inferred to have produced the two high-grade quartz-bearing assemblages are, respectively, the KFMASH divariant reaction:

$$Bt + Crd + Qtz = Grt + Kfs + L$$

(for SW2a and SW2b), and the KFMASH univariant reaction:

$$Bt + Grt + Qtz = Crd + Hyp + Kfs + L$$

(for D567 and D568). The second reaction is the upgrade univariant termination of the first (Pattison & Harte, 1985, in press; Grant, 1985). These two reactions, along with the reaction Bt + Sil + Qtz = Grt + Crd + Kfs + L, have been placed in Fig. 5 based on the estimates of Holdaway & Lee (1977), Thompson (1982), and Grant (1985). The isopleths of

TABLE 6

Geothermometry and geobarometry of high-grade quartz-bearing metapelites

		D568	*D568b*	*SW2a*	*SW2b*
Garnet	X_{Fe}	0·761	0·761	0·780	0·772
	X_{Mg}	0·169	0·165	0·140	0·153
	X_{Ca}	0·035	0·036	0·025	0·023
	X_{Mn}	0·035	0·039	0·054	0·052
Biotite	X_{Fe}	0·628	0·621	0·679	0·668
	X_{Mg}	0·372	0·379	0·321	0·332
	X^{VI}_{Al}	0·053	0·061	0·106	0·118
	X^{VI}_{Ti}	0·100	0·112	0·078	0·082
Cordierite	X_{Fe}	0·482	P	0·499	0·476
	X_{Mg}	0·518	P	0·501	0·524
Orthopyroxene	X_{Fe}	0·645	—	—	—
	X_{Mg}	0·345	—	—	—
	X^{VI}_{Al}	0·059	—	—	—
Plagioclase	X_{Ca}	0·357	0·370	0·255	0·264
	X_{Na}	0·620	0·619	0·727	0·724
T(Grt–Bt)*	HL	785	766	793	808
	FS	930	892	942	972
	HS	943	908	952	981
	IM1	745	691	784	804
	IM2	771	696	790	802
T(Grt–Crd)*	HL	792	—	753	743
T(Grt–Opx)*	H	764	—	—	—
	HG	770	—	—	—
P(Grt–Pl–Opx–Qtz)†	BWB	3·2	—	—	—
	PC	3·0	—	—	—
P(Grt–Crd–Sil–Qtz)†	NW	<3·8(4·1)‡	—	<3·6(3·9)	<3·7(4·0)
	L1	<2·9(3·3)	—	<2·9(3·3)	<3·0(3·4)
	L2	<3·6(4·0)	—	<3·6(4·0)	<3·7(4·1)
	MS	<4·2(4·8)	—	<4·0(4·6)	<4·1(4·7)

All Fe assumed to be Fe^{2+}.

* T(°C) calculated for $P = 3$ kb.

† P(kb) calculated for $T = 750$ °C.

‡ P(kb) calculated for $X^{Crd}_{HydCrd} = 0{\cdot}0$ and 0·25 (the latter in brackets).

P = pinitized cordierite. Garnet: $X_i = i/Fe + Mg + Ca + Mn$. Biotite: $X_i = i/Fe + Mg$; $X^{VI}_i = i/Al^{VI} + Ti + Fe + Mg + Mn + Ca$. Cordierite: $X_i = i/Fe + Mg$. Hypersthene: $X_i = i/Fe + Mg$; X^{VI}_{Al} = (Al calculated for six oxygens)/2. Plagioclase: $X_i = i/Na + K + Ca$. HL—Holdaway & Lee, 1977, table 7. FS—Ferry & Spear, 1978, eqn. 7. HS—Hodges & Spear, 1982, eqn. 9. IM1, IM2—Indares & Martignole, 1985, eqns. 18 and 19. H—Harley, 1984, eqn. 15. HG—Harley & Green, 1982, eqn. 5. BWB—Bohlen *et al.*, 1983, fig. 5. PC—Perkins & Chipera, 1985, eqn. 17. NW—Newton & Wood, 1979, figs. 4 and 5. L1, L2—Lonker, 1981, appendix 4, reaction (11), eqns. 1 and 2. MS—Martignole & Sisi, 1981, figs. 5 and 6.

Mg/(Mg + Fe) in cordierite from the lower-grade reactions have been extended through these reactions. Reaction 4a changes from a dehydration reaction immediately above reaction 3 to a dehydration–melting reaction (Thompson, 1982) above the vapour-saturated solidus.

Geothermometry

All temperatures have been calculated assuming a pressure of 3 kb. From Table 7, the temperature estimates concentrate between 750 and 800 °C, but range from 690 to 980 °C, showing the scatter typical of geothermometry in high-grade rocks.

It is difficult to judge which calibrations, if any, give accurate temperatures. The only independent evidence is the estimated location of the high-grade reactions in Fig. 4, which would indicate about 750 °C for the Grt + Crd + Bt + Qtz assemblages, and about 760 °C for the Grt + Hy + Crd + Qtz + Bt(?) assemblage (D568). If biotite is not in equilibrium with the rest of the assemblage in D568, then higher temperatures are possible. The calibrations which satisfy these constraints best are the Grt–Hy formulae of Harley & Green (1982) and Harley (1984), the Grt–Crd formula of Holdaway & Lee (1977), and the Grt–Bt calibrations of Holdaway & Lee (1977) and Indares & Martignole (1985).

Geobarometry

A mean temperature of 750 °C has been used for the geobarometric calculations. The selection of this temperature is not critical to the conclusions, because the geobarometer reactions have very flat slopes in P–T space.

The Grt–Sil–Crd–Qtz barometer gives a maximum pressure estimate, because sillimanite is not present in the quartz-bearing assemblages. Cordierite water contents of 0·0 and 0·25 mol are thought to bracket the expected range in these high-grade assemblages (Droop & Charnley, 1985). Averaging all calibrations, upper pressure limits of 3·6 and 4·0 kb, respectively, are obtained for the above cordierite water contents.

The Grt–Pl–Opx–Qtz barometer is in principle superior to the Grt–Sil–Pl–Qtz barometer for these rocks, because a unique pressure may be calculated, and no correction is necessary for cordierite water content. The calibrations of Bohlen *et al.*, (1983) and Perkins & Chipera (1985; Fe end member) are favoured over the calibration of Newton & Perkins (1982). The two former calibrations are based on experiments in the Fe end member system, which more closely emulates the compositions of the natural minerals than the Mg system on which Newton & Perkins (1982) is based. Consequently, uncertainties in activity–composition relations are minimized. These give pressures of 3·0 and 3·2 respectively, compared with 4·2 kb for Newton & Perkins.

The above pressure estimates are in excellent agreement with the petrogenetic grid estimate of $3{\cdot}0 \pm 0{\cdot}5$ kb, as well as the independent estimates of $2{\cdot}8 \pm 0{\cdot}4$ kb of Heuss-Assbichler & Masch (in press) and ~ 3 kb of Weiss & Troll (in press).

THE INFLUENCE OF GRAPHITE ON PELITIC PHASE RELATIONS

A number of features of the graphitic Ballachulish Slate contrast with those of the non-graphitic pelitic units. These include the exclusive development of the reaction 2a assemblage (Ms + Crd + And + Bt + Qtz) in the graphitic slates compared with the reaction 2b assemblage (Ms + Crd + Kfs + Bt + Qtz) in the non-graphitic units, and the development of reaction 1 further from the contact in the graphitic slates than in the non-graphitic pelites. Pattison (1987), in a paper on the variation in mineral assemblages and mineral chemistry in the aureole, showed that these contrasts are not due to mineral compositional differences between the units, such as Mg/(Mg + Fe), mica Al-content, or biotite F-content, nor due to other participating minerals such as carbonates. Rather, the contrasts can be explained in a simple manner by considering the composition of hydrous vapour with and without coexisting graphite.

The interaction of graphite with water introduces C-bearing fluid species into the predominantly hydrous fluid evolved during the metamorphism of the pelites (e.g., Ohmoto & Kerrick, 1977). For a given pressure and temperature, the abundances of the main C–O–H fluid species, H_2O, CO_2, CH_4, CO, and H_2, can be determined if one variable, such as f_{O_2}, is fixed (e.g., French, 1966). However, in over 95% of the pelites, both graphitic and

non-graphitic, ilmenite is the only oxide present, so that independent estimation of f_{O_2} by magnetite–ilmenite or magnetite–graphite oxybarometry is not possible. Under reducing conditions, H_2S may also be an important fluid species (e.g., Tracy & Robinson, 1988), but the absence of pyrrhotite in a number of specimens at Ballachulish appears to argue against this.

In contrast to an externally imposed f_{O_2}, Ohmoto & Kerrick (1977) argued that during dehydration reactions in graphitic pelites, the fluid is internally buffered to a composition of maximum H_2O content. This corresponds to the reaction $2C+2H_2O=CO_2+CH_4$, in which the dominant fluid species is H_2O, and CO_2 and CH_4 are in equal, but smaller, abundance. The proportion of H_2O in the maximum-H_2O fluid decreases with temperature from $X_{H_2O}=0{\cdot}90$ at 500 °C to 0·67 at 800 °C, both at 3 kb (fig. 3, Ohmoto & Kerrick, 1977). These calculations assume ideal mixing in the mixed fluid (i.e., $X_{H_2O}=a_{H_2O}$); because activity coefficients for H_2O are positive in H_2O–CO_2–CH_4 fluids (Kerrick & Jacobs, 1981), actual X_{H_2O} may be somewhat lower (see below).

Reaction 2a in the Ballachulish Slate

In addition to the exclusive development of reaction 2a in the graphitic Ballachulish Slate, the Mg/(Mg+Fe) compositions of coexisting cordierite and biotite in graphitic assemblages do not conform to the consistent pattern seen through successive assemblage zones in the non-graphitic pelites (Pattison, 1987). Referring to Fig. 6, for uniform a_{H_2O}, the Mg/(Mg+Fe) compositions of cordierite and biotite in reaction 2a should be less magnesian than on univariant reaction 3. Rather, in reaction 2a assemblages in the graphitic slate, cordierite and biotite are more magnesian than cordierite and biotite from non-graphitic pelites on univariant reaction 3 (e.g., 0·54–0·57 vs 0·50, respectively, for cordierite; see Fig. 7).

The P–T positions of reactions 1, 2a, 2b, 3, 4a, and 4b were shifted by reducing a_{H_2O} in equilibrium with graphite according to fig. 3 of Ohmoto & Kerrick (1977). Because CO_2 and CH_4 are both non-polar molecules, their effect on the activity of H_2O is comparable, so the activity model for H_2O is based on Kerrick & Jacobs (1981) Hard Sphere Modified Redlich–Kwong equations for binary H_2O–CO_2 fluids. The results are shown in Fig. 7. Because reaction 4a releases only 0·5 mol H_2O, the shift in this reaction due to lowering of a_{H_2O} is small, but in reactions 2b, 3, and 4b, the effect is significant (e.g., for reaction 3, $\sim$15 °C shift for $X_{H_2O}=0{\cdot}79$, corresponding to $a_{H_2O}=0{\cdot}84$). The result is that the Mg/(Mg+Fe) compositions of cordierite and biotite on univariant reaction 3 for graphitic pelites are displaced to more magnesian compositions by 0·06–0·07, giving cordierite an Mg/(Mg+Fe) ratio of 0·57. This is equal to or more magnesian than the compositions of the cordierite in the reaction 2a assemblages, thereby eliminating the apparent inconsistency (see Fig. 7). If H_2S is additionally present, a_{H_2O} will be lowered still further, resulting in a greater shift in Mg/(Mg+Fe).

It appears that the shift in Mg/(Mg+Fe) due to the lowering of a_{H_2O} is responsible for the exclusive development of reaction 2a in the graphitic slates. If there were no graphite present in the slates, the measured range of Mg/(Mg+Fe) compositions of cordierite and biotite would result in the development of reaction 2b rather than reaction 2a assemblages (Pattison, 1987).

Variations in the development of reaction 1 between graphitic and non-graphitic units

Another conspicuous feature of the Ballachulish Slate compared with non-graphitic units is the development further from the contact of the reaction 1 assemblage Ms+Chl

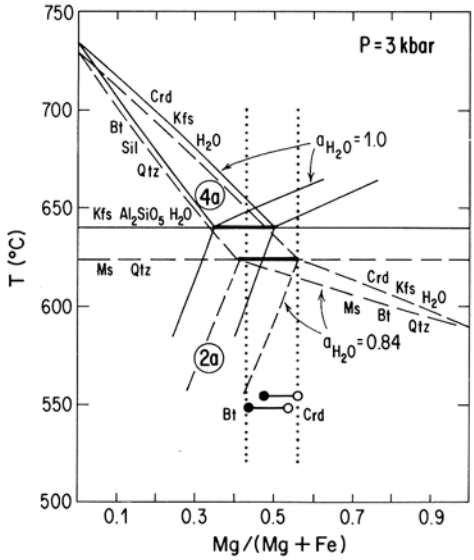

FIG. 7. Illustration of the shift to more magnesian compositions of cordierite and biotite due to lowering of a_{H_2O} in graphitic pelites (dashed lines), relative to non-graphitic pelites (solid lines). The Bt–Crd tie-lines are for reaction 2a assemblages Ms + Crd + Qtz + And + Bt in the graphitic Ballachulish Slate. The lowering of a_{H_2O} results in an expanded stability field of reaction 2a in graphitic pelites, accounting for the polarized development of this reaction in the Ballachulish Slate.

+ Crd + Bt + Qtz. Using the data described above, a T–a_{H_2O} diagram at 3 kb was calculated (see Fig. 8). Dotted on the diagram is the line of maximum a_{H_2O} of hydrous fluid in equilibrium with graphite, derived from a 3 kb isobaric section through fig. 3 of Ohmoto & Kerrick (1977). The prograde path of metamorphism for graphitic and non-graphitic pelites is shown by dashed and solid lines respectively. According to this diagram, reaction 1 commences 10–15 °C lower in graphitic pelites than in non-graphitic pelites. Although this is a small temperature interval, its effect appears to be manifested on the east flank of the aureole by the outward displacement of reaction 1 in the Ballachulish Slate relative to the Appin Phyllite (see Fig. 1). There is a less well-constrained indication of outward displacement of reaction 3 in the graphitic slates compared with the non-graphitic pelites in the southern part of the aureole.

In contrast to the effect on dehydration reactions, Fig. 8 predicts that incipient vapour-consuming partial melting would be delayed rather than promoted in the graphitic slates. Evidence for this effect is hampered by the difficulty in reliably identifying incipient anatectic migmatization in the pelites (Pattison & Harte, 1988).

EVIDENCE FOR THE ATTAINMENT OF EQUILIBRIUM IN THE AUREOLE

In contrast to regional metamorphism, which typically operates over a time scale of 10–100 Ma, contact metamorphism typically occurs over a much shorter time scale, on the order of 1 Ma or less (Spera, 1980). Buntebarth (in press), in a detailed study of the cooling history of the Ballachulish igneous complex and aureole, estimated that all rocks heated above 500 °C achieved their maximum temperature in less than 0·2 Ma. This relatively rapid rate of heating sometimes gives rise to the notion that equilibrium is not likely to be attained during contact metamorphism.

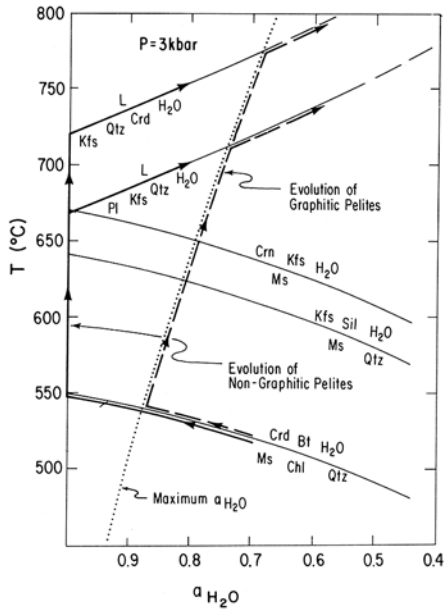

FIG. 8. Calculated 3 kb isobaric T–a_{H_2O} diagram for reactions 1, 3, and 5. The shape of the melting curves is taken from a 3 kb section through fig. 16-6 of Burnham (1979). The line of maximum a_{H_2O} is derived from a 3 kb section through fig. 3 of Ohmoto & Kerrick (1977). The dashed line shows the prograde evolution of graphitic pelites, whilst the solid line is for non-graphitic pelites. The two melting curves are for plagioclase-bearing and plagioclase-absent assemblages. The starting a_{H_2O} of 0·7 has been selected arbitrarily.

Phase rule considerations

In the Ballachulish aureole, all the evidence in the pelites suggests the attainment of gross equilibrium. If thermal aureoles were less able to achieve equilibrium than regional terrains, one might expect a disproportionately large number of low variance assemblages in contact aureoles, due to reaction overstepping. In the Ballachulish aureole, this appears not to be the case; the pelitic mineral assemblages obey the constraints of the phase rule, fitting consistently and with no overlap into the various divariant and trivariant fields of Fig. 2 (Pattison, 1987). Univariant assemblages, predicted by the phase rule to be very rare, have indeed been found in only five out of 377 thin sections. The only exception to this pattern is the overlap in the development of andalusite and sillimanite, but this situation is well known in many contact and regional settings (see earlier discussion).

In contrast, within the narrow aureole surrounding the small granodioritic stock in the southeast of the area, there is a disproportionately large number of univariant assemblages, including assemblages in which corundum and andalusite occur in Ms + Qtz-rich layers (Pattison, 1985). These And + Crn + Qtz + Ms assemblages suggest that reaction 5 (Ms = Crn + Kfs + H_2O) commenced before reaction 3 (Ms + Qtz = Al_2SiO_5 + Kfs + H_2O) went to completion. Such disequilibrium features in the narrow aureole provide a notable contrast to the well-behaved assemblages in the main aureole.

Cordierite-producing reactions

Putnis & Holland (1986) argued that substantial overstepping of experimentally determined cordierite-producing reaction boundaries would be required to nucleate natural

cordierite. This is based on their assessment that the cordierite used in the experiments was low (ordered) cordierite, in contrast to natural cordierite that nucleated as high (disordered) cordierite. For reactions 1 and 2b, they estimated 85 °C overstepping. Referring to Fig. 5, this would mean that reaction 1 would be effectively coincident with reaction 3, and reaction 2b would lie 60–70 °C higher than reaction 3.

Examining the mineral zones in the Ballachulish aureole (Fig. 1), there is no evidence for such overstepping. The sequence and spacing of the mineral zones is consistent with the equilibrium spacing of the reactions in P–T space (see Figs. 5 and 6), which include both cordierite-bearing and cordierite-absent reactions. To explain this consistency between nature and experiment, it would appear either that both the natural and experimental cordierite were ordered or else both disordered. Maresch *et al.* (in press) argued that cordierite in the Ballachulish aureole never went through an early disordered stage, instead nucleating as ordered cordierite. If this is the case, then both the experimental cordierite and the natural cordierite would appear to have been ordered.

The fact that gross equilibrium appears to have been attained during relatively rapid heating at Ballachulish supports Walther & Wood's (1984) arguments that kinetic factors do not dominate the stability of mineral assemblages formed by devolatilization reactions during contact and regional metamorphism.

CONCLUSIONS

(1) A quantitative petrogenetic grid was derived for pelitic reactions in the Ballachulish aureole. The derivation of thermodynamic data from experiments was hampered by the unknown compositions of many of the minerals in the experiments, and by apparent inconsistency between the experiments. Nevertheless, a calibrated grid was obtained that satisfies most of the data. In the calibrated grid, the first appearance of sillimanite is located between the And = Sil boundaries of Richardson *et al.* (1969) and Holdaway (1971).

(2) Using the calibrated petrogenetic grid, pressure during contact metamorphism is estimated to have been $3{\cdot}0 \pm 0{\cdot}5$ kb. The 3 kb estimate agrees to within 0·3 kb of estimates from published geobarometers and two other independent petrological studies. Temperatures ranged from 560 ± 20 °C at the first development of cordierite by reaction 1 to 750–800 °C in Grt + Crd + Hy assemblages in pelitic screens in the igneous complex.

(3) The presence of graphite in the Ballachulish Slate diluted the hydrous vapour phase with C-bearing fluid species. Lower a_{H_2O} enlarged the stability field of the andalusite-bearing assemblage And + Bt + Qtz + Ms + Crd, accounting for the exclusive development of this subzone in the graphitic slates. Lower a_{H_2O} also explains the initial development of cordierite in graphitic slates further from the igneous contacts than in non-graphitic units.

(4) Qualitative and quantitative evidence suggests that gross equilibrium was attained during contact metamorphism of the pelites, with the exception of the andalusite–sillimanite transition. There is no evidence for reaction overstepping of cordierite-producing reactions, as suggested by Putnis & Holland (1986). Given the relative brevity of the thermal metamorphic pulse at Ballachulish (<0·2 Ma; Buntebarth, in press), this supports Walther & Wood's (1984) arguments that kinetics do not significantly affect the P–T stability of mineral assemblages formed by dehydration reactions during prograde contact or regional metamorphism.

ACKNOWLEDGEMENTS

This work forms part of a Ph.D. thesis completed at the University of Edinburgh. I acknowledge the Association of Commonwealth Universities for the award of a Commonwealth Scholarship. Bernard Evans, Edgar Froese, and Jeff Grambling provided

helpful reviews. I thank Ben Harte for his careful supervision, Andy Walker for his help with the computing, and Peter Hill and Doug Russell for their help with the electron microprobe analysis at the University of Edinburgh.

REFERENCES

Bailey, E. B., & Maufe, H. B., 1960. The geology of Ben Nevis and Glen Coe and the surrounding country: explanation of Sheet 53. *Mem. Geol. Soc. Scotland.* Edinburgh: H.M.S.O., 307 pp.

Berman, R. G., 1988. Internally consistent thermodynamic data for minerals in the system Na_2O–K_2O–CaO–MgO–FeO–Fe_2O_3–Al_2O_3–SiO_2–TiO_2–H_2O–CO_2. *J. Petrology* **29,** 445–522.

Bird, G. W., & Fawcett, J. J., 1973. Stability relations of Mg-chlorite, muscovite, and quartz between 5 and 10 kb water pressure. *Ibid.* **14,** 415–28.

Bohlen, S. R., Wall, V. J., & Boettcher, A. L., 1983. Experimental investigation and application of garnet granulite equilibria. *Contr. Miner. Petrol.* **83,** 52–61.

Brown, J. F., 1975. The geochronology of northwest Argyllshire. Unpublished Ph.D. thesis, University of Oxford.

Buntebarth, G., in press. Thermal models of cooling. In: Voll, G., Topel, J., Pattison, D. R. M. & Seifert, F. (eds.) *Equilibrium and Kinetics in Contact Metamorphism: The Ballachulish Igneous Complex and its Aureole.* Heidelberg: Springer-Verlag.

Burnell, J. R., Jr., & Rutherford, M. J., 1984. An experimental investigation of the chlorite terminal equilibrium in pelitic rocks. *Am. Miner.* **69,** 1015–24.

Burnham, C. W., 1979. The importance of volatile constituents. In: Yoder, H. S. (ed.) *The Evolution of the Igneous Rocks—Fiftieth Anniversary Perspectives.* Princeton: Princeton University Press, 439–82.

Chatterjee, N. D., & Johannes, W. S., 1974. Thermal stability and standard thermodynamic properties of synthetic $2M_1$-muscovite, $KAl_2AlSi_3O_{10}(OH)_2$. *Contr. Miner. Petrol.* **48,** 89–114.

Dempster, T. J., 1985. Uplift patterns and orogenic evolution in the Scottish Dalradian. *J. Geol. Soc. Lond.* **142,** 111–28.

Droop, G. T. R., & Treloar, P. J., 1981. Pressures of metamorphism in the thermal aureole of the Etive Granite Complex. *Scot. J. Geol.* **17,** 85–102.

Evans, A. L., Mitchell, J. G., Embleton, B. J. J., & Creer, K. M., 1971. Radiometric ages of the Devonian polar shift relative to Europe. *Nature (Phys. Sci.)* **229,** 50–51.

Evans, N. H., & Speer, J. A., 1984. Low pressure metamorphism and anatexis of Carolina Slate Belt phyllites in the contact aureole of the Lilesville pluton, North Carolina. *Contr. Miner. Petrol.* **87,** 297–309.

Ferry, J. M., & Spear, F. S., 1978. Experimental calibration of the partitioning of Fe and Mg between biotite and garnet. *Ibid.* **66,** 113–18.

Fisher, J. R., & Zen, E.-An., 1971. Thermochemical calculations from hydrothermal phase equilibrium data and the free energy of H_2O. *Am. J. Sci.* **270,** 297–314.

Fleming, P. D., & Fawcett, J. J., 1976. Upper stability of chlorite + quartz in the system MgO–FeO–Al_2O_3–SiO_2–H_2O at 2 kb water pressure. *Am. Miner.* **61,** 1175–93.

French, B. M., 1966. Some geological implications of equilibrium between graphite and a C–H–O gas phase at high temperatures and pressures. *Rev. Geophys.* **4,** 223–53.

Graham, C. M., Greig, K. M., Sheppard, S. M. F., & Turi, B., 1983. Genesis and mobility of the H_2O–CO_2 fluid phase during regional greenschist and epidote amphibolite facies metamorphism: a petrological and stable isotope study in the Scottish Dalradian. *J. Geol. Soc. Lond.* **140,** 577–600.

Grant, J. A., 1985. Phase equilibria in low-pressure partial melting of pelitic rocks. *Am. J. Sci.* **285,** 409–35.

Guidotti, C. V., Cheney, J. F., & Conatore, P. D., 1975. Interrelationship between Mg/Fe ratio and octahedral Al content in biotite. *Am. Miner.* **60,** 849–53.

Harley, S. L., 1984. An experimental study of the partitioning of Fe and Mg between garnet and orthopyroxene. *Contr. Miner. Petrol.* **86,** 359–73.

—— Green, D. H., 1982. Garnet–orthopyroxene barometry for granulites and garnet peridotites. *Nature* **300,** 697–700.

Harmon, R. S., 1983. Oxygen and strontium isotopic evidence regarding the role of continental crust in the origin and evolution of the British Caledonian granites. In: Atherton, M. P., & Gribble, C. D. (eds.) *Migmatites, Melting and Metamorphism.* Nantwich: Shiva, 62–79.

Helgeson, H. C., Delaney, J. M., Nesbitt, H. W., & Bird, D. K., 1978. Summary and critique of the thermodynamic properties of rock forming minerals. *Am. J. Sci.* **278A,** 1–229.

Heuss-Assbichler, S., 1987. Mikrotexturen, Reaktionsmechanismen und Stofftransport bei Dekarbonatisierungsreaktion in Thermoaureolen. Unpublished Ph.D. thesis, Ludw.-Maxim. University, München, 191 pp.

Hirschberg, A., & Winkler, H. G. F., 1968. Stabilitatsbeziehungen zwischen Chlorit, Cordierit und Almandin bei der Metamorphose. *Beitr. Miner. Petrog.* **18,** 17–42.

Hodges, K. V., & Spear, F. S., 1982. Geothermometry, geobarometry and the Al_2SiO_5 triple point at Mt. Moosilauke, New Hampshire. *Am. Miner.* **67,** 1118–34.

Hoernes, S., MacLeod-Kinsel, S., Harmon, R. S., Pattison, D. R. M., & Strong, D. F., in press. Stable isotope geochemistry on the intrusive complex and its metamorphic aureole. In: Voll, G., Topel, J., Pattison, D. R. M. & Seifert, F. (eds.) *Equilibrium and Kinetics in Contact Metamorphism: The Ballachulish Igneous Complex and its Thermal Aureole.* Heidelberg: Springer-Verlag.

Hoffer, E., 1976. The reaction sillimanite + biotite + quartz $\rightleftharpoons$ cordierite + feldspar + H_2O and partial melting in the system K_2O–FeO–MgO–Al_2O_3–SiO_2–H_2O. *Contr. Miner. Petrol.* **55,** 127–30.

Holdaway, M. J., 1971. Stability of andalusite and the aluminum silicate phase diagram. *Am. J. Sci.* **271,** 97–131.

—— 1980. Chemical formulae and activity models for biotite, muscovite and chlorite applicable to pelitic metamorphic rocks. *Am. Miner.* **65,** 711–19.

—— Lee, S. M., 1977. Fe–Mg cordierite stability in high-grade pelitic rocks based on experimental, theoretical and natural observations. *Contr. Miner. Petrol.* **63,** 175–98.

Holland, T. J. B., & Powell, R., 1985. An internally consistent thermodynamic dataset with uncertainties and correlations: 2. Data and results. *J. Metamorphic Geol.* **3,** 343–70.

Indares, A., & Martignole, J., 1985. Biotite–garnet geothermometry in the granulite facies: the influence of Ti and Al in biotite. *Am. Miner.* **70,** 272–8.

Kerrick, D. M., 1987. Fibrolite in contact aureoles of Donegal, Ireland. *Ibid.* **72,** 240–54.

—— Jacobs, G. K., 1981. A modified Redlich–Kwong equation for H_2O, CO_2, and H_2O–CO_2 mixtures at elevated pressures and temperatures. *Am. J. Sci.* **281,** 883–916.

—— Speer, A., 1988. The role of minor element solid solution on the andalusite–sillimanite equilibrium in metapelites and paraluminous granitoids. *Ibid.* **288,** 152–92.

Kretz, R., 1983. Symbols for rock-forming minerals. *Am. Miner.* **68,** 277–9.

Labotka, T. C., Papike, J. J., & Vaniman, D. T., 1981. Petrology of contact metamorphosed argillite from the Rove Formation, Gunflint Trail, Minnesota. *Ibid.* **66,** 70–86.

Lonker, S. W., 1981. The *P–T–X* relations of the cordierite–garnet–sillimanite–quartz equilibrium. *Am. J. Sci.* **281,** 1056–90.

Marsh, B. D., 1982. On the mechanics of igneous diapirism, stoping, and zone melting. *Ibid.* **282,** 808–55.

Martignole, J., & Sisi, J. C., 1981. Cordierite–garnet–H_2O equilibrium: a geological thermometer, barometer and water fugacity indicator. *Contr. Miner. Petrol.* **77,** 38–46.

Masch, L., & Heuss-Assbichler, S., in press. Decarbonation reactions in siliceous dolomites and impure limestones. In: Voll, G., Topel, J., Pattison, D. R. M., & Seifert, F. (eds.) *Equilibrium and Kinetics in Contact Metamorphism: The Ballachulish Igneous Complex and its Aureole.* Heidelberg: Springer-Verlag.

Mirwald, P. W., & Schreyer, W., 1977. Die stabile und metastabile Abbaureaktion von Mg-Cordierit in Talc, Dishen und Quartz und ihre Abhangigkeit vom gleichwichts Wassergehalt des Cordierits. *Fortschr. Miner.* **55,** 95–7.

Newton, R. C., & Perkins, D. III, 1982. Thermodynamic calibration of geobarometers based on the assemblages garnet–plagioclase–orthopyroxene (clinopyroxene)–quartz. *Am. Miner.* **67,** 203–22.

—— Wood, B. J., 1979. Thermodynamics of water in cordierite and some petrological consequences of cordierite as a hydrous phase. *Contr. Miner. Petrol.* **68,** 391–405.

Ohmoto, H., & Kerrick, D. M., 1977. Devolatilization equilibria in graphitic systems. *Am. J. Sci.* **277,** 1013–44.

Pattison, D. R. M., 1985. Petrogenesis of pelitic rocks in the Ballachulish thermal aureole. Unpublished Ph.D. thesis, University of Edinburgh, 590 pp.

—— 1987. Variations in Mg/(Mg + Fe), F, and (Fe, Mg)Si = 2Al in pelitic minerals in the Ballachulish thermal aureole, Scotland. *Am. Miner.* **72,** 255–72.

—— Harte, B., 1985. A petrogenetic grid for pelites in the Ballachulish and other Scottish thermal aureoles. *J. Geol. Soc. Lond.* **142,** 7–28.

—— —— 1988. Evolution of structurally contrasting anatectic migmatites in the 3-kb Ballachulish aureole, Scotland, *J. Metamorphic Geol.* **6,** 475–94.

—— —— in press. Petrography and mineral chemistry of metapelites. In: Voll, G., Töpel, J., Pattison, D. R. M., & Seifert, F. (eds.) *Equilibrium and Kinetics in Contact Metamorphism: The Ballachulish Igneous Complex and its Aureole.* Heidelberg: Springer-Verlag.

—— Voll, G., in press. Regional geology of the Ballachulish area. In: Voll, G., Töpel, J., Pattison, D. R. M., & Seifert, F. (eds.) *Equilibrium and Kinetics in Contact Metamorphism: The Ballachulish Igneous Complex and its Aureole.* Heidelberg: Springer-Verlag.

Perkins, D. III, & Chipera, S. J., 1985. Garnet–orthopyroxene–plagioclase–quartz barometry; refinement and application to the English River subprovince and the Minnesota River Valley. *Contr. Miner. Petrol.* **89,** 69–80.

Powell, R. 1978. *Equilibrium Thermodynamics in Petrology; An Introduction.* London: Harper & Row, 284 pp.

—— Evans, J. A., 1983. A new geobarometer for the assemblage biotite–muscovite–chlorite–quartz. *J. Metamorphic Geol.* **1,** 331–6.

Putnis, A., & Holland, T. J. B., 1986. Sector trilling in cordierite and equilibrium overstepping in metamorphism. *Contr. Miner. Petrol.* **93,** 265–72.

Richardson, S. W., Gilbert, M. C., & Bell, P. M., 1969. Experimental determination of kyanite–andalusite and andalusite–sillimanite equilibria: the aluminum silicate triple point. *Am. J. Sci.* **267,** 259–72.

Robie, R. A., Hemingway, B. S., & Fisher, J. R., 1978. Thermodynamic properties of minerals and related substances at 298·15 K and 1 bar (10^5 pascals) pressure and at higher temperature. *U.S. Geol. Surv. Bull.* **1452,** 456 pp.

Schreyer, W., & Yoder, H. S., 1964. The system Mg-cordierite–H_2O and related rocks. *Neues Jahrb. Miner. Abh.* **101,** 271–342.

Seifert, F., 1970. Low temperature compatibility relations of cordierite in haplopelites of the system K_2O–MgO–Al_2O_3–SiO_2–H_2O. *J. Petrology* **11,** 73–99.

—— 1976. Stability of the assemblage cordierite + K-feldspar + quartz. *Contr. Miner. Petrol.* **57,** 179–85.

Spear, F. S., & Cheney, J. T., 1989. A petrogenic grid for pelitic schists in the system SiO_2–Al_2O_3–FeO–MgO–K_2O–H_2O. *Ibid.* **101,** 149–64.

Spera, F., 1980. Thermal evolution of plutons: a parameterized approach. *Science* **207,** 299–301.

Thompson, A. B., 1976. Mineral reactions in pelitic rocks. II Calculation of some *P–T–X* (Fe–Mg) phase relations. *Am. J. Sci.* **276,** 425–54.

—— 1982. Dehydration melting of pelitic rocks and the generation of H_2O-undersaturated granitic liquids. *Ibid.* **282,** 1567–95.

—— Tracy, R. J., 1979. Model systems for anatexis of pelitic rocks: II. Facies series and reactions in the system CaO–$KAlO_2$–$NaAlO_2$–Al_2O_3–SiO_2–H_2O. *Contr. Miner. Petrol.* **70,** 429–38.

Tracy, R. J. 1982. Compositional zoning and inclusions in metamorphic minerals. In: Ferry, J. M. (ed.) *Characterization of Metamorphism through Mineral Equilibria. Min. Soc. Am., Reviews in Mineralogy* **10,** 762–75.

—— Robinson, P. 1988. Silicate–sulfide–oxide–fluid reactions in granulite-grade pelitic rocks, Central Massachusetts. *Am. J. Sci.* **288A,** 45–74.

Voll, G., Topel, J., Pattison, D. R. M., & Seifert, F., in press. *Equilibrium and Kinetics in Contact Metamorphism: The Ballachulish Igneous Complex and its Thermal Aureole.* Heidelberg: Springer-Verlag.

Walther, J. V., & Wood, B. J., 1984. Rate and mechanism in prograde metamorphism. *Contr. Miner. Petrol.* **88,** 246–59.

Weiss, S., 1986. Petrogenese des Intrusivkomplexes von Ballachulish, Westschottland: Kristallisationsverlauf in einem zonierten Kaledonischen Pluton. Unpublished Ph.D. thesis, Lud.-Maxim. University, München, 228 pp.

—— Troll, G., 1989. The Ballachulish Igneous Complex, Scotland: petrography, mineral chemistry, and order of crystallization in the monzodiorite–quartz diorite suite and in the granite. *J. Petrology* **30,** 1069–116.

—— —— in press. Thermal conditions and crystallization sequence in the Ballachulish Complex. In: Voll, G., Topel, J., Pattison, D. R. M., & Seifert, F. (eds.) *Equilibrium and Kinetics in Contact Metamorphism: The Ballachulish Igneous Complex and its Aureole.* Heidelberg: Springer-Verlag.